

Overexpression of Mucin 13 due to Promoter Methylation Promotes Aggressive Behavior in Ovarian Cancer Cells

Hye Youn Sung,¹ Ae Kyung Park,² Woong Ju,³ and Jung-Hyuck Ahn¹

Departments of ¹Biochemistry and ²Obstetrics and Gynecology, School of Medicine, Ewha Womans University, Seoul;

³College of Pharmacy, Suncheon National University, Suncheon, Korea.

Received: January 20, 2014

Revised: February 19, 2014

Accepted: March 7, 2014

Co-corresponding authors: Dr. Jung-Hyuck Ahn,
Department of Biochemistry,
School of Medicine, Ewha Womans University,
1071 Anyangcheon-ro, Yangcheon-gu,
Seoul 158-710, Korea.

Tel: 82-2-2650-5712, Fax: 82-2-2652-7846

E-mail: ahnj@ewha.ac.kr and

Dr. Woong Ju,

Department of Obstetrics and Gynecology,
School of Medicine, Ewha Womans University,
1071 Anyangcheon-ro, Yangcheon-gu,
Seoul 158-710, Korea.

Tel: 82-2-2650-2779, Fax: 82-2-2647-9860

E-mail: goodmorning@ewha.ac.kr

The authors have no financial conflicts of interest.

Purpose: Recent discoveries suggest that aberrant DNA methylation provides cancer cells with advanced metastatic properties. However, the precise regulatory mechanisms controlling metastasis genes and their role in metastatic transformation are largely unknown. To address epigenetically-regulated gene products involved in ovarian cancer metastasis, we examined the mechanisms regulating mucin 13 (MUC13) expression and its influence on aggressive behaviors of ovarian malignancies. **Materials and Methods:** We injected SK-OV-3 ovarian cancer cells peritoneally into nude mice to mimic human ovarian tumor metastasis. Overexpression of *MUC13* mRNA was detected in metastatic implants from the xenografts by expression microarray analysis and quantitative reverse-transcription polymerase chain reaction (qRT-PCR). The DNA methylation status within the *MUC13* promoter region was determined using bisulfite sequencing PCR and quantitative methylation-specific PCR. We evaluated the effects of exogenous MUC13 on cell invasion and migration using *in vitro* transwell assays. **Results:** *MUC13* mRNA expression was up-regulated, and methylation of specific CpG sites within the promoter was reduced in the metastatic implants relative to those in wild-type SK-OV-3 cells. Addition of a DNA methyltransferase inhibitor to SK-OV-3 cells induced *MUC13* expression, thereby implying epigenetic regulation of *MUC13* by promoter methylation. MUC13 overexpression increased migration and invasiveness, compared to control cells, suggesting aberrant up-regulation of *MUC13* is strongly associated with progression of aggressive behaviors in ovarian cancer. **Conclusion:** We provide novel evidence for epigenetic regulation of *MUC13* in ovarian cancer. We suggest that the DNA methylation status within the *MUC13* promoter region may be a potential biomarker of aggressive behavior in ovarian cancer.

Key Words: Ovarian cancer, mouse xenograft, MUC13, DNA methylation

© Copyright:

Yonsei University College of Medicine 2014

This is an Open Access article distributed under the terms of the Creative Commons Attribution Non-Commercial License (<http://creativecommons.org/licenses/by-nc/3.0>) which permits unrestricted non-commercial use, distribution, and reproduction in any medium, provided the original work is properly cited.

INTRODUCTION

Ovarian cancer is the most lethal gynecological malignancy. The high mortality of this cancer can be explained by the fact that greater than 70% of ovarian cancer patients are first diagnosed at advanced stages¹ due to the lack of reliable biomarkers for early detection and predominantly asymptomatic early-stage disease. De-

spite progress in surgical treatments and chemotherapy, the overall survival rate still remains low.² Therefore, a better understanding of the molecular mechanisms that contribute to the aggressive behavior of ovarian cancer would be useful to identify new therapeutic targets and biomarkers for early detection and prediction of cancer treatment response.

Mucins are macromolecular glycoproteins produced by epithelial cells. Mucins are characterized by numerous tandem repeat-domains rich in proline and serine and/or threonine residues linked to a large number of O-glycans.^{3,4} Under normal physiological conditions, mucins function as a physical barrier that protects epithelial cells from pathogens, toxins, and harsh environments.³⁻⁵ Mucins are also involved in proliferation, differentiation, cell-cell adhesion, and immunosuppression of epithelial cells by transmitting external signals to epithelial cells in response to alterations in the local molecular environment.^{4,5} Alterations in expression and protein modifications, including glycosylation, of mucins have been implicated in tumorigenicity and metastasis of a variety of cancers, such as colon cancer,⁶ pancreatic cancer,⁷ breast cancer,^{8,9} and ovarian cancer.¹⁰⁻¹² In particular, overexpression of various mucins (MUC1, MUC2, MUC3, MUC4, MUC 5AC, MUC13, and MUC16) has been reported in many epithelial ovarian cancers, compared with normal ovarian surface epithelium and benign ovarian tumors.^{4,13} Although it is necessary to improve its sensitivity and specificity, mucin 16 (MUC16), which encodes the CA125 antigen, is currently used as a serum marker to diagnose ovarian cancer.^{14,15} Other differentially expressed mucins, including MUC1¹⁶ and MUC4,¹⁷ have also been suggested as potential biomarkers for early ovarian cancer detection and prognosis.

In the present study, we overexpressed *MUC13* in human ovarian carcinoma peritoneal xenografts and explored the mechanisms regulating *MUC13* expression. We report novel epigenetic regulation of *MUC13* and examine its influence on aggressive phenotypes of ovarian cancer.

MATERIALS AND METHODS

Cell culture

The human ovarian cancer cell line SK-OV-3 was purchased from the American Type Culture Collection (ATCC no. HTB-77) and cultured in McCoy's 5A medium (Gibco/BRL, Rockville, MD, USA) containing 10% fetal bovine serum (Gibco/BRL), 100 U/mL penicillin (Gibco/BRL),

and 100 µg/mL streptomycin (Gibco/BRL) in a 95% humidified air and 5% CO₂ atmosphere at 37°C.

Ovarian cancer mouse xenograft model

All procedures for handling and euthanizing the animals in this study were performed in strict compliance with the guidelines of the Korean animal protection law and approved by the Institutional Animal Care and Use Committee of Ewha Womans University School of Medicine. SK-OV-3 cells (2×10⁶) suspended in culture media were intraperitoneally injected into 10 female nude mice (BALB/c, 4–6 weeks old). Four weeks after inoculation, the xenograft mice were sacrificed, and at least four implants adhering to the mesothelial surface of each mouse were harvested.

RNA preparation and quantitative reverse-transcription polymerase chain reaction (qRT-PCR)

Total RNA was extracted from the metastatic implants of ovarian cancer mouse xenografts and SK-OV-3 cells using the RNeasy mini kit (Qiagen, Valencia, CA, USA) according to the manufacturer's protocol. One microgram of total RNA was converted to cDNA using Superscript II reverse transcriptase (Invitrogen, Carlsbad, CA, USA) and oligo-(dT)₁₂₋₁₈ primers (Invitrogen) according to the manufacturer's instructions. Quantitative reverse-transcription polymerase chain reaction (qRT-PCR) was performed in a 20-µL reaction mixture containing 1 µL cDNA, 10 µL SYBR Premix EX Taq (Takara Bio, Otsu, Japan), 0.4 µL Rox reference dye (50x, Takara Bio), and 200 nM primers for each gene. The primer sequences were: *MUC13* (forward), 5'-AGAAACATTC CATGGCCTATCAA-3'; *MUC13* (reverse), 5'-TGTCCA TAAACAGATGTGCCAAA-3'; *GAPDH* (forward), 5'-AAT CCCATCACCATCTTCCA-3'; and *GAPDH* (reverse), 5'-TGGACTCCACGACGTACTCA-3'. The reactions were run on a 7500 fast real-time PCR system (Applied Biosystems, Foster City, CA, USA) at 95°C for 30 s, followed by 40 cycles of 95°C for 3 s and 60°C for 30 s, and a single dissociation cycle of 95°C for 15 s, 60°C for 60 s, and 95°C for 15 s. All PCR reactions were performed in triplicate, and the specificity of the reaction was detected by melting-curve analysis at the dissociation stage. Comparative quantification of each target gene was performed based on cycle threshold (C_T) normalized to *GAPDH* using the $\Delta\Delta C_T$ method.

Messenger RNA microarray chip processing and analysis of gene expression data

Total RNA was extracted from the harvested metastatic-im-

plants of ovarian cancer mouse xenografts and SK-OV-3 cells using the RNeasy mini kit (Qiagen), and one microgram of total RNA was amplified and labeled according to the Affymetrix GeneChip Whole Transcript Sense Target Labeling protocol. The resulting labeled cDNA was hybridized to Affymetrix Human Gene 1.0 ST arrays (Affymetrix, Santa Clara, CA, USA). The scanned raw expression values were background corrected, normalized, and summarized using the Robust Multiarray Averaging approach in the Bioconductor “affy” package (Affymetrix). The resulting log₂-transformed data were used for further analyses.

To identify differentially expressed genes (DEGs), we applied moderated t-statistics based on an empirical Bayesian approach.¹⁸ Significantly up-regulated and down-regulated DEGs were defined as genes with at least a twofold difference in expression level between the xenograft cells and the wild-type SK-OV-3 cells after correction for multiple testing (Benjamini-Hochberg false-discovery rate-adjusted *p*-value <0.05).¹⁹ Finally, we excluded genes with a low expression level (maximum log₂ expression level in a total of eight samples <7.0) from the list of DEGs. The Database for Annotation, Visualization and Integrated Discovery (DAVID) bioinformatics resource was used to detect overrepresented the gene ontology (GO) clusters from the identified DEGs.²⁰

Bisulfite sequencing PCR (BSP)

Genomic DNA was extracted from the harvested metastatic-implant of ovarian cancer mouse xenografts and SK-OV-3 cells using the QIAmp DNA mini kit (Qiagen) according to the manufacturer's protocol. Bisulfite treatment of genomic DNA was performed using the EpiTect Bisulfite Kit (Qiagen) according to the manufacturer's instructions. For bisulfite sequencing of the target promoter region of *MUC13*, bisulfite sequencing PCR (BSP) was carried out using conventional PCR in a 50 µL reaction mixture containing 10 ng bisulfite-modified genomic DNA, 1.5 mM MgCl₂, 200 µM dNTP, 1 U Platinum Taq polymerase (Invitrogen), 1X Platinum Taq buffer, and 200 nM specific BSP forward and reverse primers for each gene. The BSP primers were designed using the MethPrimer software (<http://www.urogene.org/methprimer>). For *MUC13*, the BSP product was 413 bp (position in the human GRCh37/hg19 assembly: chr3 124653578–124653990) and contained six CpG sites. The BSP primer sequences were: (forward), 5'-ATTTGAGGAGGAAATGATTTTTTTT-3'; and (reverse), 5'-CCTCT

TCAAAAATTCTCAAACTACA-3'. The reaction ran at 95°C for 5 min, followed by 30 cycles of 95°C for 30 s, 50–55°C for 30 s, and 72°C for 30 s, and a final elongation step at 72°C for 5 min.

The BSP products were purified using the QIAquick Gel Extraction kit (Qiagen) according to the manufacturer's protocols and ligated into the yT&A cloning vector (Yeastern Biotech, Taipei, Taiwan). The ligation products were used to transform competent DH5a *Escherichia coli* cells (RBC Bioscience, Taipei, Taiwan) using standard procedures. Blue/white screening was used to select bacterial clones, and BSP product-positive clones were confirmed by colony PCR using the BSP primers to verify the insert size. Plasmid DNA was then extracted from at least 15 insert-positive clones using the QIAprep Spin Miniprep kit (Qiagen) and sequenced using M13 primer to analyze the methylation status at specific CpG sites.

Quantitative methylation-specific PCR (qMSP)

Quantitative methylation-specific PCR (qMSP) was carried out with bisulfite-modified genomic DNA as the template and specific primer sequences designed to detect the methylated and unmethylated forms of *MUC13*. The following methylated/unmethylated-specific primers were used: (methylated forward), 5'-GGGTATAAAGTTTAGTTATT AATTGAC-3'; (unmethylated forward), 5'-GGGTATAA AGTTTAGTTATTAATTGAT-3'; and (reverse), 5'-AAAA TCCTAACTTATTTTAAACTTTAAATC-3'. For qMSP, 20 µL reaction mixture containing 2 µL (10–100 ng/µL) bisulfite-treated DNA, 10 µL SYBR Premix EX Taq (Takara Bio), 0.4 µL Rox reference dye (50x Takara Bio), and 200 nM each primer were reacted using a 7500 fast real-time PCR system (Applied Biosystems). The amplification reaction conditions were: 95°C for 30 s, followed by 40 cycles of 95°C for 3 s and 58°C for 30 s. The PCR product was then reacted at 95°C for 15 s, 60°C for 1 min, and 95°C for 15 s to examine the specificity. Methylation and nonmethylation of the specific CpG sites were calculated as follows (Ct represents the threshold cycle):

$$\text{Percent methylation} = 100 / [1 + 2^{(\Delta C_{\text{meth}} - \Delta C_{\text{nonmeth}})}]$$

The treatment of 5-aza-2'-deoxycytidine (5-aza-dC)

To demethylate methylated CpG sites, SK-OV-3 cells were treated with increasing concentrations (0, 5, and 10 µM) of 5-aza-2'-deoxycytidine (5-aza-dC) (Sigma-Aldrich, St. Louis, MO, USA) for 3 days. The media was replaced daily.

Transient transfection

To establish a transient expression system, SK-OV-3 cells were transfected with pCMV6-XL5-MUC13 (Origene, Rockville, MD, USA) or pEGFP-N3 (Clontech, Mountain View, CA, USA) plasmid DNAs using Lipofectamine™ 2000 (Invitrogen). Briefly, the cells were plated at a density of 6×10^5 cells/well in six-well plates and allowed to grow overnight. Two micrograms of each plasmid DNA and 5 μ L of Lipofectamine™ 2000 were diluted separately in Opti-Mem medium to a total volume of 250 μ L. The diluted plasmid DNAs and Lipofectamine™ 2000 were mixed and incubated at room temperature for 20 min to generate the transfection mixtures. The cells were washed with serum-free McCoy's 5A medium, and then the transfection mixtures were added to each well of the six-well plates containing complete growth medium and incubated at 37°C for 24 h in a 5% CO₂ incubator.

Transwell migration and *in vitro* invasion assay

After 24 h of transfection, the transfected cells were starved by serum deprivation. The cell migration assay was performed in 24-well Transwell plates containing inserts with a polycarbonate membrane with an 8.0 μ m pore size (Corning, New York, USA). After 24 h of serum deprivation, the cells were detached from the plates and resuspended in serum-free medium at a density of 2×10^6 cells/mL. One hundred microliters of the SK-OV-3 cell suspension was added to the upper compartment of the transwell chamber. For each experiment, both chemotactic migration to medium containing 15% fetal bovine serum (FBS) and random migration in serum-free medium were assessed in parallel Transwell plates for 6 h at 37°C in a 5% CO₂ incubator.

The *in vitro* invasion assay was performed using a BD BioCoat Matrigel Invasion Chamber (Becton-Dickinson, Franklin Lakes, NJ, USA). After 24 h of serum deprivation, SK-OV-3 cells were detached from the plates and resuspended in serum-free medium at a density of 1×10^6 cells/mL. One hundred microliters of the SK-OV-3 cell suspension was added to the upper compartment of the invasion chamber, and 500 μ L McCoy's 5A medium containing 10% FBS was added to the lower compartment of the chamber. The migration through the Matrigel chamber was allowed to proceed at 37°C for 24 h in a 5% CO₂ incubator. After the incubation period, the cells that had not migrated from the upper side of the filter were carefully scraped away with cotton swabs. The cells on the lower side of the filter were fixed for 2 min using Diff-Quick kit solution (Thermo Fisher Scientific, Waltham,

MA, USA), stained with 1% crystal violet for 2 min, and washed twice with distilled water at room temperature. The images of the stained cells on the lower side of the membrane were acquired at 200 \times magnification in six different fields. For quantitative analysis, the stained cells were subsequently extracted with 10% acetic acid, and colorimetric measurement was performed at 590 nm.

RESULTS

MUC13 expression is increased in the ovarian carcinoma xenografts

Ovarian carcinoma SK-OV-3 cells were injected into the peritoneal cavities of female nude mice. Four weeks after inoculation, dense solid tumors formed in the intestine, liver, and omentum were harvested from seven mice. We analyzed their expression profiles in comparison to wild-type SK-OV-3 cells using expression microarray. The microarray results revealed alterations of mRNA expression of more than two-fold in 937 genes, including 444 up-regulated genes and 529 down-regulated genes. Among the 444 up-regulated genes, *MUC13* mRNA expression was highly over-expressed (2.3–11.2-fold) in the metastatic implants from ovarian carcinoma xenografts, compared to wild-type SK-OV-3 cells (Fig. 1A). To validate the microarray results, we performed qRT-PCR. The qRT-PCR results also revealed significantly higher *MUC13* mRNA expression (1.7–6.1-fold) in implants from the xenografts, compared to wild-type SK-OV-3 cells (Fig. 1B).

The *MUC13* promoter regions from the ovarian carcinoma xenografts are aberrantly hypomethylated

We investigated whether DNA methylation status was altered within the *MUC13* promoter region in ovarian metastatic implants, compared to SK-OV-3 cells. We chose two ovarian metastatic implants to investigate: one with the smallest change in *MUC13* mRNA expression (1C) and the other with the largest change in *MUC13* mRNA expression (2C) (Fig. 1).

The *MUC13* promoter region (124653578–124653990 in chromosome 3) was PCR amplified using bisulfite-modified genomic DNA as a template to obtain 413 bp bisulfite PCR products in the ovarian metastatic implants and wild-type SK-OV-3 cells. The DNA methylation patterns of each PCR product were determined by sequencing analyses. Our results showed that promoter CpGs are hypomethylated in

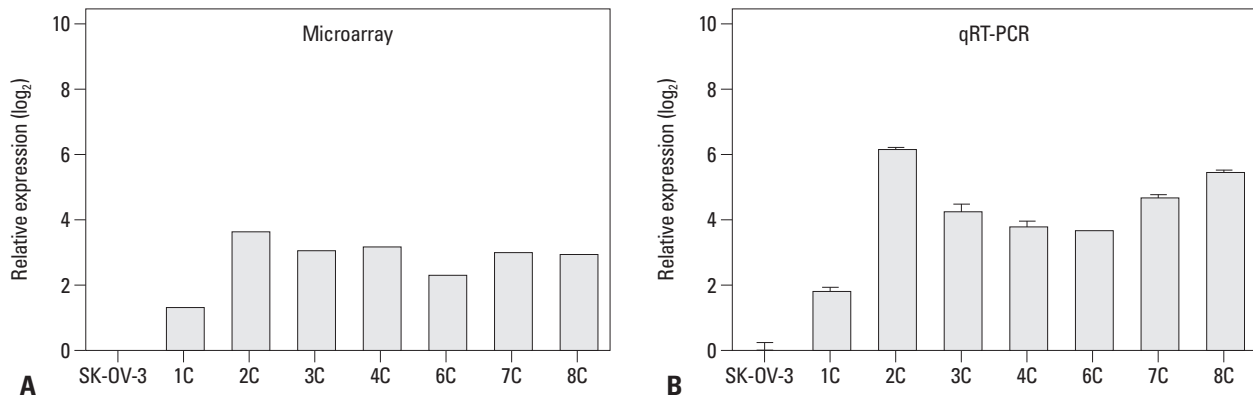


Fig. 1. *MUC13* expression is up-regulated in metastatic implants from xenograft mice. *MUC13* mRNA expression was measured by expression microarray (A) and qRT-PCR (B). The error bars indicate means \pm standard deviation of triplicate experiments. The metastatic implants from each mouse xenograft are labeled 1C–8C (n=7). qRT-PCR, quantitative reverse-transcription polymerase chain reaction.

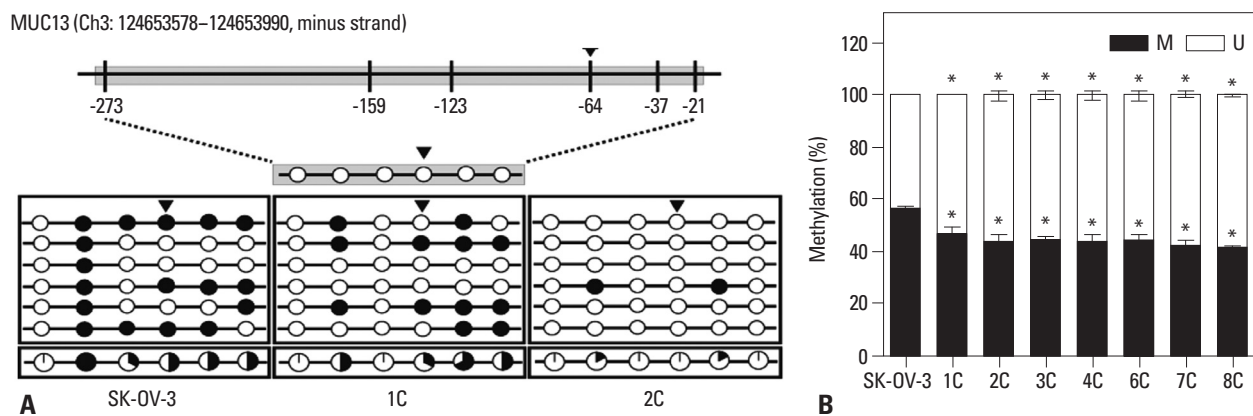


Fig. 2. DNA methylation is altered at CpG sites in the *MUC13* promoter in metastatic implants from mouse xenografts. The DNA methylation status was analyzed using Bisulfite sequencing analysis (A). The *MUC13* promoter region is located at positions 124653578–124653990 in the human GRCh37/hg19 assembly and contains six CpG residues within chromosome 3. The six CpGs are located at positions -273, -159, -123, -64, -37, and -21 from the transcription start site. Each circle represents CpG dinucleotides. The methylation status of each CpG site is illustrated by black (methylated) and white (unmethylated) circles, and the total percentage of methylation at each site is indicated by a pie graph on the bottom line. The black segment of the pie graph indicates the methylated CpG percentage, whereas the white segment represents the unmethylated CpG percentage. The DNA methylation status at the -64 CpG site was analyzed using qMSP (B). Triangles above the circles in A indicate the specific CpG site used for qMSP. Data are shown as the means \pm SD (n=3). Statistical analyses were performed using a one-way ANOVA and subsequent Bonferroni tests (* p <0.05). M, the percentage of methylated CpGs; U, the percentage of unmethylated CpGs; qMSP, quantitative methylation-specific PCR; PCR, polymerase chain reaction; ANOVA, analysis of variance.

both ovarian metastatic implant samples, compared to SK-OV-3 cells, particularly at -159, -123, and -64 CpGs (Fig. 2A). In addition, the CpG methylation status in implant 2C was demethylated at all six tested CpGs, compared to implant 1C and wild-type SK-OV-3 cells (Fig. 2A).

Further analyses of DNA methylation patterns using MSP also revealed significantly lower methylation at -64 CpG in the ovarian metastatic implants (n=7), compared to SK-OV-3 cells (Fig. 2B).

DNA methylation regulates *MUC13* expression

To determine whether altered *MUC13* mRNA expression is regulated by DNA methylation of the promoter CpGs, we treated SK-OV-3 cells with the DNA methyltransferase inhibitor 5-aza-dC. After treatment with 0, 5, and 10 μ M 5-aza-dC, decreased methylation activity at -64 CpG site

was confirmed using MSP (Fig. 3A). Furthermore, *MUC13* mRNA expression was significantly increased in a dose-dependent manner (Fig. 3B).

MUC13 overexpression correlates with aggressive phenotypes of ovarian cancer cells

To explore the function of *MUC13*, we examined the effects of *MUC13* on *in vitro* migration and invasion using transwell chambers. SK-OV-3 cells were transfected with full length *MUC13* or enhanced green fluorescent protein cDNAs. *MUC13* overexpression in transfected cells was confirmed using qRT-PCR (data not shown). We observed increased migration capacity of *MUC13*-transfected cells, compared to mock-transfected cells (Fig. 4A and B). For invasion assays, Matrigel-coated transwell chambers were used. As shown in Fig. 4, the number of invasive cells was

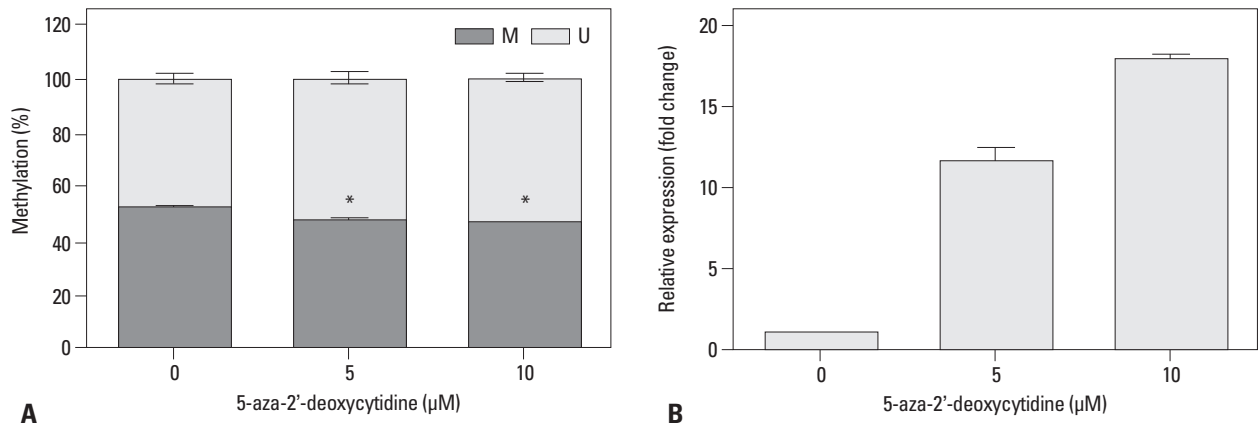


Fig. 3. *MUC13* expression changes following demethylation in SK-OV-3 cells. The SK-OV-3 cells were treated for 3 days with 0, 5, and 10 μM 5-aza-2'-deoxycytidine, respectively. After treatment with 5-aza-2'-deoxycytidine, the DNA methylation status at the -64 CpG site of *MUC13* was analyzed using qMSP (A), and *MUC13* mRNA expression was measured by qRT-PCR (B). Data are shown as the means±SD (n=3). Statistical analyses were performed using a one-way ANOVA and subsequent Bonferroni tests (* $p<0.05$). M, the percentage of methylated CpG; U, the percentage of unmethylated CpG; qMSP, quantitative methylation-specific PCR; qRT-PCR, quantitative reverse-transcription polymerase chain reaction; ANOVA, analysis of variance.

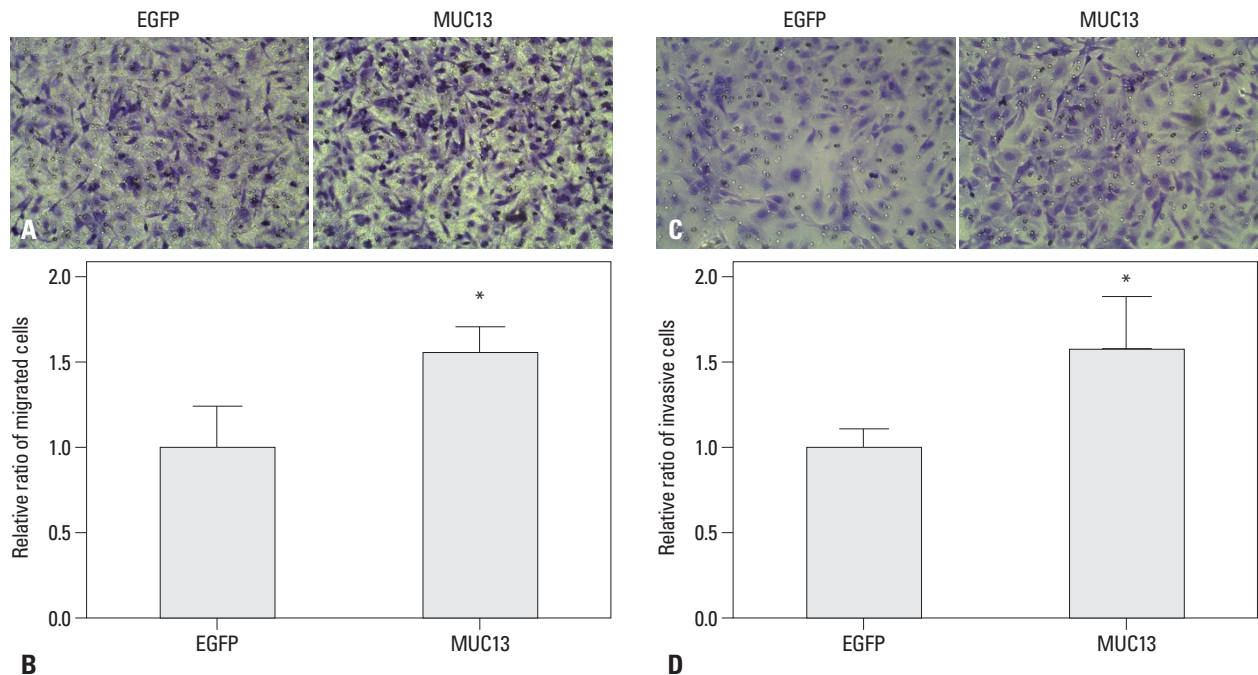


Fig. 4. *MUC13* promotes migration and invasiveness of SK-OV-3 cells. Migration of serum-starved cells towards 15% serum-containing medium was determined by the transwell assay. Cells that migrated through an 8-μm pore filter were fixed and stained with crystal violet. Representative images of migrated cells transfected with EGFP or *MUC13* are shown (A). Quantitative analysis of migrated cells was carried out by measuring the absorbance of extracts of cell stains at 595 nm. Data are shown as means±SD for triplicate measurements (B). Statistical analysis was performed using a t-test (* $p<0.05$). Invasion by serum-starved cells towards 10% serum-containing medium was determined using a Matrigel-coated invasion chamber. The cells invading through the Matrigel were fixed and stained with crystal violet. Representative images of invading cells transfected with EGFP or *MUC13* are shown (C). Quantitative analysis of invading cells was carried out by measuring the absorbance of extracts of cell stains at 595 nm. Data are shown as means±SD for triplicate measurements (D). Statistical analysis was performed using a t-test (* $p<0.05$). EGFP, enhanced green fluorescent protein.

markedly increased in *MUC13*-transfected cells, compared to mock-transfected cells (Fig. 4C and D).

DISCUSSION

MUC13 is a member of the membrane-associated mucin family and is commonly expressed in the trachea, kidney,

esophagus, and gastrointestinal tract.^{18,19} The *MUC13* glycoprotein is composed of a large 151-amino acid tandem repeat domain in the NH₂-terminus that is highly O-glycosylated on serine and threonine residues. The degree and nature of glycosylation in this domain affects cell adhesion to the extracellular matrix and cell-cell interactions.¹⁹ The central region of *MUC13* consists of a 23-amino acid transmembrane domain and three epithelial growth factor (EGF)-like

domains that may potentially interact with EGF receptors to modulate ovarian cancer cell proliferation via epidermal growth factor receptor (EGFR) signaling pathways.¹³ The carboxyl (COOH)-terminus contains a 69-amino acid cytoplasmic domain that contains several potential phosphorylation sites and a protein kinase C phosphorylation motif,¹⁹ further suggesting that MUC13 may function as a signaling molecule.

Aberrant MUC13 overexpression has been demonstrated in colon cancer,^{6,20} gastric cancer,²¹ pancreatic cancer,²² and ovarian cancer.¹³ However, the regulatory mechanisms of MUC13 expression have not yet been elucidated. Our results showed that *MUC13* mRNA expression is aberrantly up-regulated, with reduced methylation of specific CpG sites within its promoter in metastatic implants, compared to wild-type SK-OV-3 cells (Figs. 1 and 2). Treatment of wild-type SK-OV-3 cells with the DNA methyltransferase inhibitor 5-aza-2'-deoxycytidine dose-dependently enhanced *MUC13* expression, thus implying epigenetic regulation of *MUC13* by promoter methylation (Fig. 3). We also discovered that MUC13 overexpression increases migration and invasiveness, suggesting aberrant MUC13 up-regulation is strongly associated with progression of aggressive behavior in ovarian cancer cells (Fig. 4). Aberrant increased expression of MUC13 in ovarian cancer tissues, compared with normal ovary/benign tissues, has been previously demonstrated.¹³ In agreement with our results, Chauhan, et al.¹³ also reported that gain of functional MUC13 in ovarian cancer cells significantly increased cell motility, proliferation, and tumorigenesis in a xenograft mouse model system. However, DNA methylation-dependent epigenetic regulation of *MUC13* has not been investigated in ovarian cancer. In this study, we demonstrated that *MUC13* could be a novel metastasis-promoting gene that enhances the metastatic phenotype in ovarian cancer via epigenetic transcriptional regulation.

In conclusion, the results of the present study provide novel evidence for epigenetic regulation of *MUC13* in ovarian cancer and suggest MUC13 influences the aggressive behavior of ovarian cancer. Although further clinical research is required, our findings suggest that the DNA methylation status within the *MUC13* promoter region may be a potential biomarker of aggressiveness in ovarian cancer.

ACKNOWLEDGEMENTS

This study was supported by a grant of the Korean Health

Technology R&D Project, Ministry of Health & Welfare, Republic of Korea (HI12C0050) and RP-Grant 2011 of Ewha Womans University.

REFERENCES

1. Lengyel E. Ovarian cancer development and metastasis. *Am J Pathol* 2010;177:1053-64.
2. Kipps E, Tan DS, Kaye SB. Meeting the challenge of ascites in ovarian cancer: new avenues for therapy and research. *Nat Rev Cancer* 2013;13:273-82.
3. Rose MC, Voynow JA. Respiratory tract mucin genes and mucin glycoproteins in health and disease. *Physiol Rev* 2006;86:245-78.
4. Singh AP, Senapati S, Ponnusamy MP, Jain M, Lele SM, Davis JS, et al. Clinical potential of mucins in diagnosis, prognosis, and therapy of ovarian cancer. *Lancet Oncol* 2008;9:1076-85.
5. Hollingsworth MA, Swanson BJ. Mucins in cancer: protection and control of the cell surface. *Nat Rev Cancer* 2004;4:45-60.
6. Gupta BK, Maher DM, Ebeling MC, Sundram V, Koch MD, Lynch DW, et al. Increased expression and aberrant localization of mucin 13 in metastatic colon cancer. *J Histochem Cytochem* 2012;60:822-31.
7. Ringel J, Löhr M. The MUC gene family: their role in diagnosis and early detection of pancreatic cancer. *Mol Cancer* 2003;2:9.
8. Brockhausen I, Yang JM, Burchell J, Whitehouse C, Taylor-Papadimitriou J. Mechanisms underlying aberrant glycosylation of MUC1 mucin in breast cancer cells. *Eur J Biochem* 1995;233:607-17.
9. Rakha EA, Boyce RW, Abd El-Rehim D, Kurien T, Green AR, Paish EC, et al. Expression of mucins (MUC1, MUC2, MUC3, MUC4, MUC5AC and MUC6) and their prognostic significance in human breast cancer. *Mod Pathol* 2005;18:1295-304.
10. Rosen DG, Wang L, Atkinson JN, Yu Y, Lu KH, Diamandis EP, et al. Potential markers that complement expression of CA125 in epithelial ovarian cancer. *Gynecol Oncol* 2005;99:267-77.
11. Dong Y, Walsh MD, Cummings MC, Wright RG, Khoo SK, Parsons PG, et al. Expression of MUC1 and MUC2 mucins in epithelial ovarian tumours. *J Pathol* 1997;183:311-7.
12. Giuntoli RL 2nd, Rodriguez GC, Whitaker RS, Dodge R, Voynow JA. Mucin gene expression in ovarian cancers. *Cancer Res* 1998;58:5546-50.
13. Chauhan SC, Vannatta K, Ebeling MC, Vinayek N, Watanabe A, Pandey KK, et al. Expression and functions of transmembrane mucin MUC13 in ovarian cancer. *Cancer Res* 2009;69:765-74.
14. Canney PA, Moore M, Wilkinson PM, James RD. Ovarian cancer antigen CA125: a prospective clinical assessment of its role as a tumour marker. *Br J Cancer* 1984;50:765-9.
15. Yin BW, Dnistrian A, Lloyd KO. Ovarian cancer antigen CA125 is encoded by the MUC16 mucin gene. *Int J Cancer* 2002;98:737-40.
16. Budiu RA, Mantia-Smaldone G, Elishaev E, Chu T, Thaller J, McCabe K, et al. Soluble MUC1 and serum MUC1-specific antibodies are potential prognostic biomarkers for platinum-resistant ovarian cancer. *Cancer Immunol Immunother* 2011;60:975-84.
17. Chauhan SC, Singh AP, Ruiz F, Johansson SL, Jain M, Smith LM, et al. Aberrant expression of MUC4 in ovarian carcinoma: diagnostic significance alone and in combination with MUC1 and

- MUC16 (CA125). *Mod Pathol* 2006;19:1386-94.
18. Williams SJ, Wreschner DH, Tran M, Eyre HJ, Sutherland GR, McGuckin MA. Muc13, a novel human cell surface mucin expressed by epithelial and hemopoietic cells. *J Biol Chem* 2001; 276:18327-36.
 19. Maher DM, Gupta BK, Nagata S, Jaggi M, Chauhan SC. Mucin 13: structure, function, and potential roles in cancer pathogenesis. *Mol Cancer Res* 2011;9:531-7.
 20. Walsh MD, Young JP, Leggett BA, Williams SH, Jass JR, McGuckin MA. The MUC13 cell surface mucin is highly expressed by human colorectal carcinomas. *Hum Pathol* 2007;38:883-92.
 21. Shimamura T, Ito H, Shibahara J, Watanabe A, Hippo Y, Taniguchi H, et al. Overexpression of MUC13 is associated with intestinal-type gastric cancer. *Cancer Sci* 2005;96:265-73.
 22. Chauhan SC, Ebeling MC, Maher DM, Koch MD, Watanabe A, Aburatani H, et al. MUC13 mucin augments pancreatic tumorigenesis. *Mol Cancer Ther* 2012;11:24-33.